Published in final edited form as:
Clin Exp Metastasis. 2014 December ; 31(8): 945–959. doi:10.1007/s10585-014-9682-1.

Wnt signaling induces gene expression of factors associated with bone destruction in lung and breast cancer

Rachelle W. Johnson[1,2,3], **Alyssa R. Merkel**[1,3,4], **Jonathan M. Page**[5], **Nazanin S. Ruppender**[3,5], **Scott A. Guelcher**[3,5], and **Julie A. Sterling**[1,2,3]

[1]Department of Veterans Affairs: Tennessee Valley Healthcare System (VISN 9), Nashville, Tennessee, United States

[2]Department of Cancer Biology, Vanderbilt University, Nashville, Tennessee, United States

[3]Vanderbilt Center for Bone Biology, Vanderbilt University, Nashville, Tennessee, United States

[4]Department of Medicine, Vanderbilt University, Nashville, Tennessee, United States

[5]Department of Chemical and Biomolecular Engineering, Vanderbilt University, Nashville, Tennessee, United States

Abstract

Parathyroid hormone-related protein (PTHrP) is an important regulator of bone destruction in bone metastatic tumors. Transforming growth factor-beta (TGF-β) stimulates PTHrP production in part through the transcription factor Gli2, which is regulated independent of the Hedgehog signaling pathway in osteolytic cancer cells. However, inhibition of TGF-β *in vivo* does not fully inhibit tumor growth in bone or tumor-induced bone destruction, suggesting other pathways are involved. While Wnt signaling regulates Gli2 in development, the role of Wnt signaling in bone metastasis is unknown. Therefore, we investigated whether Wnt signaling regulates Gli2 expression in tumor cells that induce bone destruction. We report here that Wnt activation by β-catenin/T-cell factor 4 (TCF4) over-expression or lithium chloride (LiCl) treatment increased Gli2 and PTHrP expression in osteolytic cancer cells. This was mediated through the TCF and Smad binding sites within the Gli2 promoter as determined by promoter mutation studies, suggesting cross-talk between TGF-β and Wnt signaling. Culture of tumor cells on substrates with bone-like rigidity increased Gli2 and PTHrP production, enhanced autocrine Wnt activity and led to an increase in the TCF/Wnt signaling reporter (TOPFlash), enriched β-catenin nuclear accumulation, and elevated Wnt-related genes by PCR-array. Stromal cells serve as an additional paracrine source of Wnt ligands and enhanced Gli2 and PTHrP mRNA levels in MDA-MB-231 and RWGT2 cells *in vitro* and promoted tumor-induced bone destruction *in vivo* in a β-catenin/Wnt3a-dependent mechanism. These data indicate that a combination of matrix rigidity and stromal-secreted factors stimulate Gli2 and PTHrP through Wnt signaling in osteolytic breast cancer cells, and there is significant cross-talk between the Wnt and TGF-β signaling pathways. This suggests that the Wnt signaling pathway may be a potential therapeutic target for inhibiting tumor cell

Please address correspondence to: Julie A. Sterling, Ph.D., Vanderbilt University Medical Center, 2215B Garland Avenue, Medical Research Building IV, Room 1235, Nashville, TN 37232, Phone: 615-322-4364, Julie.sterling@vanderbilt.edu.

response to the bone microenvironment and at the very least should be considered in clinical regimens targeting TGF-β signaling.

Keywords

Gli; PTHrP; Osteolysis; Breast cancer; Matrix; Stiffness; Rigidity; Bone Metastasis

Introduction

Breast and lung cancer cells frequently metastasize to distant organs such as the bone, where they can disrupt normal bone remodeling and induce significant damage to the skeleton [1, 2]. While there have been significant advances in identifying key regulators of tumor-induced bone disease [2], the mechanisms driving the establishment of tumor cells in bone and the initiation of osteolysis remains unclear.

Upon metastasis to bone, breast and lung tumor cells up-regulate their expression of the transcription factor Gli2, which directly promotes the production and secretion of parathyroid hormone-related protein (PTHrP) into the tumor-bone microenvironment [2]. The release of PTHrP and other osteoclast-promoting factors stimulates bone resorption, enabling the release of active transforming growth factor-beta (TGF-β) from the mineralized bone matrix [1, 2]. Previous reports have indicated that TGF-β positively regulates tumor-derived Gli2 and PTHrP expression [3–5], and stimulates tumor cell proliferation in bone [1].

There are many driving forces that influence tumor cell evolution both in the breast and bone, and it is well-established that matrix rigidity is a key factor that regulates the invasive potential of breast tumor cells at the primary site of disease [6–8]. There is increasing evidence that matrix rigidity has a significant impact on tumor cell behavior in the mineralized bone microenvironment, where the stiffness encountered by the breast tumor cells is at least six orders of magnitude higher than those in the breast tissue [2, 9]. The rigidity of the mineralized bone matrix has been shown to enhance mRNA and protein levels of Gli2, PTHrP, and TGF-β ligand (all genes that facilitate cancer growth in bone) in breast and lung cancer cells through mechanotransduction [10].

Sequencing of the Gli2 promoter identified a Smad-binding element (SBE) and TCF-binding element (TBE) in a regulatory region upstream of the transcription initiation site in keratinocytes [11] establishing a physiological role for both the TGF- β and Wnt signaling pathways as regulators of Gli2. There is ample evidence that Wnt signaling in the breast drives tumor cell growth and invasiveness [12] and clinical data supports this with correlations between genetic alterations in Wnt signaling pathway molecules and patient prognosis [13]; however, the role of Wnt signaling in promoting cancer cell growth in bone has not been explored.

While autocrine signaling is an important source of Wnt activation in cancer [12, 13], paracrine signaling also contributes to the regulation of tumor invasiveness and metastasis. Studies characterizing breast tumor-stroma interactions at the primary site have identified

Wnt signaling as an essential step in metastatic colonization [14]. Cancer associated fibroblasts (CAFs) have been shown to enhance prostate cancer growth by secreting Wnt ligands [15] and exosomes that promote breast cancer cell invasion and metastasis by activating autocrine Wnt-planar cell polarity signaling [16].

We, therefore, hypothesized that Wnt signaling, both autocrine and paracrine, in addition to TGF-β signaling, drives Gli2 expression in breast and lung cancer cells that induce bone destruction. The data presented here indicate that downstream Wnt signaling molecules facilitate Gli2 and PTHrP up-regulation, and that this induction occurs 1) following tumor cell culture on substrates with bone-like rigidity, and 2) following exposure to Wnts secreted by human bone marrow stromal cells.

Methods

Cells

The human breast cancer cell line MDA-MB-231 was obtained from American Type Culture Collection (ATCC; Manassas, VA, USA) and a bone metastatic variant generated in our lab was used for all *in vitro* and *in vivo* experiments, as previously published [17, 18]. RWGT2 non-small cell lung carcinoma cells were generated in the Mundy lab [19]. The human bone marrow stromal cell line HS5 and weakly metastatic human MCF-7 breast cancer cells were obtained from ATCC. MDA-MB-231, HS5, and MCF-7 cells were maintained in Dulbecco's modified Eagle's medium (DMEM; Cell-gro, Manassas, VA, USA) plus 10% fetal bovine serum (FBS; Hyclone Laboratories, Logan UT, USA) and 1% penicillin/streptomycin (P/S; Mediatech, Manassas, VA, USA) and RWGT2 cells were maintained in Minimum Essential Medium alpha (MEMα; Cell-gro, Manassas, VA, USA) plus 10% FBS and 1% P/S. All cell lines are routinely tested for changes in cell growth and gene expression. MDA-MB-231 cells were transiently transfected with either TOPFlash, β-catenin/T-cell factor 4 (TCF4), Gli2 WT, mSmad (mS), or mTCF4 (mT) Gli2 promoter [11], or the 1.1kb PTHrP promoter [20] by lipofectamine transfection reagent and plus reagent (Invitrogen, Carlsbad, CA, USA) as previously described [4].

Human bone marrow stromal cells (BMSCs) were collected from a de-identified normal patient bone marrow aspirate kindly provided Dr. Ginger Holt with ethical consent. Cells were isolated by differential trypsinization, which enriches for the fibroblast population, and cultured for 2–3 weeks *in vitro* prior to injection *in vivo*. These cells were characterized as vimentin and α-smooth muscle actin positive (data not shown).

LiCl/sclerostin/2G7 treatments

Lithium chloride solution (LiCl, 8M solution; Sigma-Aldrich, St. Louis, MO) was added at a final concentration of 20mM [21, 22] or 40mM [21] to serum-free DMEM for 24 hours. Sclerostin (R&D Systems) was added at a final concentration of 1.5 μg/ml to DMEM or HS5 culture medium as indicated in the figure legends and incubated for 24 hours, then conditioned medium was removed and transferred to MDA-MB-231 cells for 24 hour incubation prior to RNA harvest. 2G7, a TGF-β neutralizing monoclonal antibody (provided

by the Vanderbilt Antibody Core), or control IgG 12CA5 were administered *in vitro* at 10μg/ml using the same method as sclerostin treatment.

Substrates

Tissue culture polystyrene and polyacrylamide hydrogels were employed to examine the effects of substrate rigidity on Wnt signaling in 2D *in vitro* culture. To facilitate cell adhesion and ensure that the surface chemistry was constant for all substrates tested, fibronectin (Fbn) was adsorbed to the surface of the substrates by incubating them in a 4μg/mL solution of Fbn in PBS at 4°C overnight. Polyacrylamide (PA) hydrogels were synthesized by copolymerizing a 10% solution of acrylamide and bis-acrylamide in water via free-radical polymerization using a redox pair of initiators [tetramethyl ethylene diamine (TEMED) and 10% ammonium persulphate (APS) in water]. Additionally, acrylic acid N-hydrosuccinimide (NHS) ester was copolymerized to the surface of the gels. The NHS-acrylate layer was then allowed to react with a solution of Fbn in HEPES. To measure the surface concentration of Fbn, coated substrates were incubated in a solution of Fbn antibody (1:1000) followed by incubation with a secondary HRP-conjugated antibody. The relative amount of adsorbed antibody was then quantified by reaction with 2'-azino-bis(3-ethylbenzthiazoline-6-sulphonic acid) (ABTS) and subsequent optical density reading at 405nm. All PUR and PAA substrates were prepared at the same surface concentration of Fbn that yielded an optical density of 0.12 absorbance units cm^{-2}.

Quantitative real-time RT-PCR (qPCR)

RNA was extracted using RNeasy mini kit (Qiagen), and cDNA was synthesized using Superscript III (Life Technologies), per manufacturer's instructions. Control cDNA was serially diluted to create a standard curve, and combined with TaqMan Universal PCR Master Mix (Life Technologies), and one of the following primers: TaqMan PTHLH (Hs00174969_m1), TaqMan Gli2 (Hs00257977_m1), or TaqMan Euk 18S rRNA (4352930-0910024; Applied Biosystems). Samples were loaded onto an optically clear 96-well plate (Applied Biosystems) and cycle conditions were as follows: 50°C for 2min, 95°C for 10min, (95°C for 15sec, 60°C for 1min) ×40 cycles on the 7500 Real-Time PCR System (Applied Biosystems). qPCR reactions were quantified using the 7500 Real-Time PCR Systems software (Applied Biosystems).

PCR array

MDA-MB-231 cells were seeded onto compliant PA gels or rigid TCPS coated with fibronectin (to aid with attachment) at 1.92×10^6 cells/well for 24 hours and RNA extracted as above. cDNA was synthesized from 1μg RNA per manufacturer's instructions for the RT^2Profiler PCR Array System for Wnt Signaling (SABiosciences, Frederick, MD, USA). Samples were loaded onto pre-coated 96-well array plates and reverse transcription was performed on the 7300 Real-Time PCR System (Applied Biosystems) with the following cycle conditions: 95°C for 10min, (95°C for 15sec, 60°C for 1min) × 40. Dissociation step conditions: (95°C for 15sec, 60°C for 1min, 95°C for 15sec). Reactions were quantified using 7300 Real-Time PCR Systems software by ddCT method, per manufacturer's instructions (SABiosciences). Commercial SYBR primers (Qiagen) for real-time PCR

validation are listed in table 1. Cycling conditions were (95°C for 10:00), (95°C for :30, 58°C for 1:00, 72°C for :30) × 40 cycles, followed by dissociation step (95°C for 1:00, 55°C for :30, 95°C for :30), as previously published [23].

β-catenin nuclear/cytoplasmic fractionation

MDA-MB-231 cells were seeded onto compliant PA gels, TCPS, or TCPS coated in fibronectin (TCPS+Fbn) at 1.92×10^6 cells/well and harvested for cell pellets after 24 hours incubation. Pellets were washed 2X with 1XPBS and fractionated into cytoplasmic and nuclear fractions using the NE-PER Nuclear and Cytoplasmic Extraction Reagents (Pierce/Thermo Scientific, Rockford, IL, USA), per manufacturer's instructions. Briefly, the cellular membrane was disrupted using lytic buffer to expose the cytoplasmic proteins, which were immediately harvested and stored at −80°C. The remaining nuclear fraction was recovered and lysed to yield the nuclear protein fraction, which was immediately harvested and stored at −80°C.

Western blot

Equal protein concentrations (5μg) were prepared for loading with Laemmli sample buffer and electrophoresis was performed on SDS-PAGE Mini-Protein II ready gels (Bio-Rad). Proteins were transferred to polyvinylidene fluoride (PVDF) membrane and blocked with 1XTBS containing 1% Tween 20 (1XTBST) + 5% blocking grade dry milk (Bio-Rad; Hercules, CA, USA) for 1 hour at room temperature. β-catenin antibody (BD Transduction Laboratories, Bedford, MA, USA) was added at 1:1000 dilution in blocking buffer overnight at 4°C, and the membrane was probed for 1 hour at room temperature in secondary antibody. Following detection, the membrane was stripped using Restore Western Blot Stripping Buffer (Thermo Scientific, Rockford, IL, USA), washed with 1XTBST, and re-probed with a 1:5000 dilution of β-actin antibody (Sigma-Aldrich, St. Louis, MO, USA) as a loading control.

Promoter activation/luciferase assay

Gli2 and PTHrP promoter activation was evaluated by the Dual-Luciferase Reporter Assay System (Promega, Madison, WI, USA), per manufacturer's instructions. MDA-MB-231 cells and RWGT2 cells were transfected as above and sample lysates were read for relative luminescence on a Synergy 2 plate-reader (BioTek, Winooski, VT, USA) and analyzed for subsequent fold change over control vector. All samples were normalized to an internal Renilla luciferase control.

Animals

All animal experiments were conducted with prior approval from Vanderbilt University Institutional Animal Care and Use Committee and were conducted according to NIH guidelines. In the first study, HS5 cells and MDA-MB-231 or RWGT2 cells stably transfected with either shCTNNB1 (β-Catenin) or shSCR (scrambled control) plasmid (SantaCruz) were used for all animal experiments. 250,000 tumor cells or 200,000 tumor cells + 50,000 stromal cells were injected into the tibia of 4–6 week old athymic nude mice (Harlan). Tumor progression was monitored by weekly x-ray imaging on a XR-60 digital

radiography system (Faxitron) at 35kVp for 8 sec. Mice were sacrificed at 21 days post tumor cell inoculation and hindlimbs were harvested for *ex vivo* analysis.

For the second study, 4–6 week old female nude mice were inoculated with 250,000 MDA-MB-231 cells as previously published to induce osteolytic bone destruction *in vivo* [24] or 200,000 MDA-MB-231 cells + 50,000 human BMSCs via intratibial injection (MDA-MB-231 n=9 mice, MDA-MB-231+BMSC n=7 mice). Mice were radiographically imaged once/week for 4 weeks post-tumor cell inoculation (Faxitron LX-60) at 35kVp for 8 seconds and a consistent region of interest within the proximal tibia was analysed for bone destruction using Metamorph (Molecular Devices, Incs) as previously described[4].

Histology

Hind limbs were dissected at sacrifice, fixed in 10% formalin for 48 hours, and decalcified in EDTA for 2 weeks as previously described [17, 25]. Bone sections were stained with tartrate resistant acid phosphatase (TRAP) and analyzed using ROI measurements in Osteomeasure as previously described [25].

WNT ligand ELISA

After 24 hour incubation, conditioned media was harvested from HS5 cells grown on tissue culture plates and treated with either 1.5 μg/ml sclerostin or PBS. Conditioned media was added to high binding EIA/RIA 96-well ELISA plates (Corning Life Sciences) at a 1:10 dilution and allowed to adhere overnight at 4°C. A serial dilution of WNT1, WNT 3a, and WNT5a protein was also added to generate a standard curve (25ng/ml – 0ng/ml) for use in quantitative analysis. Plates were washed in PBS + 0.5% Tween-20, and non-specific binding was blocked with 3% bovine serum albumin (BSA) in PBS + 0.5% Tween-20. Primary antibody was added for 1 hour at room temperature at the following dilutions: WNT1 1:1000, WNT3a 1:5000, WNT5a, 1:10000. HRP conjugated anti-mouse or anti-rabbit secondary antibodies (Santa Cruz Biotechnology) were added for 1 hour at room temperature at a 1:1000 dilution. OPD reagent was added per manufacture's instruction and absorbance was read at 450nm on a Synergy2 plate reader. All WNT antibodies and control protein were purchased from Abcam.

shRNA-mediated knockdown of β-catenin and Wnt3a

MDA-MB-231 or RWGT2 cells were stably transfected with shRNA for either human β-Catenin (CTNNB1, shCTNNB1) or control shRNA plasmid (scrambled control, shSCR) and HS5 cells were stably transfected with shRNA for either human WNT3A (shWNT3a) or control shRNA plasmid (scrambled control, shSCR; Santa Cruz). For each transfection, 1μg shRNA plasmid was incubated with 5μL shRNA Plasmid Transfection Reagent (Santa Cruz, sc-108061) for 45 minutes at room temperature. The cells were incubated in 200μL of the shRNA plasmid/transfection reagent mixture with 0.8 mL transfection medium (Santa Cruz) for 5 hours in a 37°C, 5% CO_2 incubator.

After incubation, DMEM plus 20% heat inactivated FBS and 2% penicillin/streptomycin was added to the cells for an additional 24 hours. Cells were harvested by trypsin for mRNA

analysis to verify knockdown. Cells were maintained in DMEM plus 10% heat inactivated FBS, 1% penicillin/streptomycin and 3μg/mL Puromycin.

Statistical analyses

All statistical analyses were performed using InStat version 3.03 software (GraphPad Software, Inc.), and n=3 biological replicates for all experiments unless indicated otherwise in the figure legend. Columns represent mean/group + standard error of the mean (SEM), and p-values were determined using unpaired Student's t-test or ANOVA as indicated in figure legends, where *p< 0.05, **p< 0.01, ***p<0.001, and ****p<0.0001.

Results

Activation of Wnt signaling stimulates Gli2 and PTHrP transcription in highly metastatic cancer cells known to induce bone destruction

Human RWGT2 lung cancer cells and MDA-MB-231 breast cancer cells, which normally express low levels of β-catenin even when plated on TCPS [26], and weakly metastatic MCF-7 breast cancer cells were transiently co-transfected with a non-degradable form of β-catenin and its co-factor TCF4 to determine the effect of downstream Wnt signaling molecules on Gli2 and PTHrP mRNA induction. Over-expression of β-catenin/TCF4 significantly increased Gli2 and PTHrP mRNA levels by qPCR in both RWGT2 (Fig. 1A&B) and MDA-MB-231 cells (Fig. 1C&D), and significantly activated the PTHrP promoter region in RWGT2 (Fig. 1E) and MDA-MB-231 cells (Fig. 1F). Gli2 promoter activity was also increased in MDA-MB-231 cells (Fig. 1F) and modestly increased (non-significant) in RWGT2 cells (Fig. 1E). In MCF7 human adenocarcinoma cells, over-expression of β-catenin significantly inhibited PTHrP promoter activation and trended toward an inhibition of the Gli2 promoter (Fig. 1G), suggesting that the stimulatory effects of downstream Wnt signaling on Gli2 and PTHrP are specific for highly metastatic cells known to induce bone destruction.

LiCl treatment, which has been previously reported to up-regulate the Wnt signaling pathway by inhibiting GSK3-β phosphorylation of β-catenin [22], significantly stimulated the Gli2 and PTHrP promoter regions in RWGT2 cells (Fig. 2A). Mid-range treatment with LiCL (20mM) increased PTHrP promoter activity in MDA-MB-231 cells, but this activation was lost with 40mM treatment (Fig. 2B). Wnt activation via LiCl treatment did not significantly affect Gli2 promoter activity in MDA-MB-231 cells (Fig. 2B) or Gli2 or PTHrP promoter activity in MCF-7 cells (Fig. 2C).

Wnt and TGF-β co-regulation of the Gli2 promoter

There is ample evidence that the TGF-β and Wnt signaling pathways crosstalk, both during development [27] and in cancer cells [28]. To this end, we examined the inter-dependence of Wnt and TGF-β signaling on Gli2 promoter activity in MDA-MB-231 cells using a construct in which the Smad binding element (SBE) or TCF binding element (TBE) located within the Gli2 promoter has been mutated (mS or mT, respectively) [11]. When the SBE was mutated, forced expression of Smad3 had no effect on Gli2 promoter activation as anticipated (Fig. 3A). Surprisingly, over-expression of β-catenin no longer modestly stimulated the Gli2

promoter as in Figure 1F, but rather inhibited Gli2 promoter activity when the SBE was mutated (Fig. 3A), indicating Wnt signaling induction of Gli2 may be dependent on downstream TGF-β signaling. When the TBE was mutated, forced expression of β-catenin did not alter Gli2 promoter activity as anticipated, and Smad3 was able to activate the Gli2 promoter despite the absence of a functional TBE (Fig. 3B), indicating that TGF-β signaling activation of the Gli2 promoter does not require the TBE.

Substrate rigidity activates autocrine Wnt signaling in breast cancer cells

Previous studies have shown that Wnt and mechanically transduced signaling cross-talk through Src kinase activity [29, 30], and that matrices with bone-like rigidity enhance Gli2 and PTHrP expression through alterations in TGF-β signaling [9, 10]. Therefore, rigidity may also influence Wnt signaling upstream of Gli2 and PTHrP, which may be important in the context of breast cancer metastasis to bone. To test this, MDA-MB-231 cells were seeded onto substrates representative of breast tissue [Compliant-polyacrylamide (PA) gel containing fibronectin (Fbn) to facilitate cell attachment] or trabecular bone [rigid tissue culture polysterene (TCPS) + Fbn or without Fbn to rule it out as a confounding factor], as previously published [10]. MDA-MB-231 cells exhibited a >1.5 fold increase in TOPflash activity, a TCF/Wnt signaling reporter, within 4 hours of seeding onto rigid substrates (Fig. 4A), and a 7-fold increase in TOPFlash activity within 24 hours when compared to cells plated on compliant PA gels (Fig. 4B), regardless of fibronectin. It was noted that baseline TOPflash activity was significantly higher at 4 hours post-seeding compared to 24 hours post-seeding.

MDA-MB-231 cells seeded onto rigid TCPS for 24 hours also exhibited greater Wnt signaling activity in a Wnt Signaling PCR-based microarray (SABiosciences) compared to cells seeded onto compliant PA gels through enhanced expression of numerous Wnt signaling molecules (Table 1). Validation of Wnt signaling molecules identified in the array are presented in Table 1.

Furthermore, MDA-MB-231 cells seeded onto rigid TCPS or TCPS + Fbn substrates showed abundant β-catenin expression in both cytosolic and nuclear fractions, while cells seeded onto compliant PA gels showed a marked decrease (by approximately 50%) in β-catenin nuclear accumulation (Fig. 4C).

Stromal cells are a source of Wnt ligands and stimulate Gli2 and PTHrP mRNA levels

To determine whether stromal cells secrete detectable levels of Wnt ligands and therefore provide a paracrine source of these proteins, conditioned media from the human bone marrow stromal cell line HS5 was evaluated for the secretion of canonical (Wnt3a, Wnt1) and non-canonical (Wnt5a) Wnt ligands. Wnt3a, Wnt1, and Wnt5a proteins were all detected in naïve fibroblasts, with the secretion of non-canonical Wnt5a notably lower than both Wnt3a and Wnt1 (Fig. 5A). Treatment with sclerostin, a potent Wnt inhibitor that binds to LRP5/6, significantly reduced Wnt3a secretion by fibroblasts, but did not significantly alter Wnt1 or Wnt5a protein levels (Fig. 5A), suggesting Wnt ligands may be differentially regulated at the receptor level. Treatment of MDA-MB-231 cells with the Wnt inhibitor sclerostin reduced basal Gli2 mRNA levels (Fig. 5B) when cells were cultured in un-

conditioned media. Treatment of MDA-MB-231 cells with 100% HS5-conditioned media (CM), a human bone marrow stromal cell line, significantly increased Gli2 mRNA levels, and this effect was ablated by the addition of sclerostin (Fig. 5B), indicating the effects of HS5-conditioned media on Gli2 stimulation are mediated entirely via Wnt signaling. Treatment with a TGF-β neutralizing monoclonal antibody 2G7 was not sufficient to reduce endogenous Gli2 mRNA levels, but abolished the stimulatory effect of HS5 CM, as did combined treatment of sclerostin+2G7 (Fig. 5B). Similarly, sclerostin treatment significantly inhibited PTHrP mRNA levels in MDA-MB-231 cells when cells were cultured in un-conditioned media (Fig. 5C). HS5-conditioned media increased PTHrP mRNA levels, and this effect was blocked by the addition of sclerostin. Treatment with 2G7 alone was not enough to significantly block HS5 CM-mediated increases in PTHrP mRNA levels, but combination of sclerostin+2G7 significantly reduced PTHrP mRNA levels (Fig. 5C). Sclerostin treatment did not significantly reduce endogenous β-catenin levels in MDA-MB-231 cells (Fig. 5D), likely due to the already low mRNA levels in these cells. HS5 CM dramatically increased β-catenin mRNA levels, and this was blocked by the addition of sclerostin. 2G7 and 2G7+sclerostin also blocked HS5 CM induction of β-catenin mRNA levels (Fig. 5D).

In order to determine whether β-catenin in tumor cells is required for HS5 CM to increase Gli2 mRNA levels, MDA-MB-231 cells expressing stable knockdown of β-catenin (CTNNB1) or scrambled control (SCR) shRNA (Fig. 6A) were treated with HS5 CM. In control MDA-MB-231 cells Gli2 mRNA levels were elevated following HS5 treatment, but this stimulatory effect was blocked in the MDA-MB-231-shCTNNB1 cells (Fig. 6B). Similarly, PTHrP mRNA levels and β-catenin mRNA levels were dramatically elevated following HS5 CM treatment in the MDA-MB-231 control cells only (Fig. 6C&D), indicating β-catenin is required for HS5 stimulation of Gli2 and PTHrP in tumor cells. A similar effect on Gli2 and PTHrP mRNA levels was observed in RWGT2 cells (data not shown). In order to verify that it is indeed Wnts secreted by HS5 cells that stimulate Gli2 and PTHrP expression in tumor cells, WNT3a, which is abundantly secreted by stromal cells (Fig. 5A) was stably knocked down in HS5 stromal cells (Fig. 6E) and CM was collected from these cells. When MDA-MB-231 cells were treated with HS5 CM from HS5 control cells, Gli2 (Fig. 6F), PTHrP (Fig. 6G) and β-catenin (Fig. 6H) mRNA levels significantly increased. The stimulatory effect of the HS5 CM was completely ablated when Wnt3a was knocked down in HS5 cells (Fig. 6F–H), indicating that Wnt3a in particular is the Gli2 and PTHrP-promoting factor produced by stromal cells. Endogenous PTHrP mRNA levels were also significantly decreased when MDA-MB-231 cells were cultured with HS5 CM with WNT3a knockdown (Fig. 6G).

Stromal cells promote tumor-induced bone destruction in a Wnt-dependent mechanism

In order to determine whether stromal cells enhance MDA-MB-231 and RWGT2 tumor-induced bone destruction and whether this is dependent on Wnt signaling, HS5 stromal cells were co-inoculated with either MDA-MB-231 or RWGT2 cells containing knockdown of β-catenin (β-catenin mRNA levels in RWGT2 shSCR = 0.617+0.011, RWGT2 shCTNNB1 = 0.071+0.002, *$p<0.05$) directly into the tibia and tumor-induced bone destruction was monitored over the course of 3 weeks. Osteolytic bone destruction was significantly greater

in the MDA-MB-231 + HS5 tumor-bearing bones compared to the control MDA-MB-231 tumor-bearing bones. Deletion of β-catenin in MDA-MB-231 cells did not significantly impact bone destruction when injected alone, but blocked the ability of HS5 cells to enhance bone destruction *in vivo* (Fig. 7A). Similarly, HS5 cells significantly enhanced RWGT2 tumor-induced bone destruction, and this effect was blocked by knockdown of β-catenin in RWGT2 cells (Fig. 7B). β-catenin knockdown alone did not significantly affect RWGT2-induced bone destruction. Importantly, deletion of WNT3a in HS5 cells significantly reduced the ability of MDA-MB-231 cells to induce bone destruction (Fig. 7C), indicating that the mechanism by which stromal cells promote tumor-induced bone destruction is dependent on Wnt signaling in tumor cells, and Wnt3a in particular secreted by stromal cells.

To determine whether primary human bone marrow stromal cells could also enhance tumor-induced osteolysis, MDA-MB-231 cells were cultured in conditioned media from primary human bone marrow stromal cells (BMSCs), which resulted in significantly greater PTHrP mRNA levels in MDA-MB-231 cells *in vitro* (Fig. 7D). Co-inoculation of MDA-MB-231 cells with primary human BMSCs significantly enhanced osteolytic lesion area *in vivo* over the course of 4 weeks (Fig. 7E).

Discussion

The work presented here demonstrates that Wnt signaling activation stimulates Gli2 and PTHrP production in tumor cells, and that there are multiple sources of Wnt signals in the tumor-bone microenvironment. Matrix rigidity activated autocrine Wnt signaling at the transcription and protein level in breast cancer cells, and BMSCs (1) provided a paracrine source of Wnt ligands, (2) stimulated Gli2 and PTHrP *in vitro* and (3) enhanced osteolytic bone destruction *in vivo*. Interestingly, Wnt activation of the Gli2 promoter required an intact Smad binding site, suggesting TCF and Smads may interact at the molecular level to regulate Gli2 transcription (Fig. 8).

Although we have previously demonstrated that Gli2 is necessary for PTHrP production *in vivo* [4], constitutive expression of β-catenin did not stimulate the GLI2 promoter in RWGT2 cells, but dramatically increased Gli2 mRNA levels. While it is possible that Wnt signaling may have GLI2-independent effects on PTHrP transcription in these cells, it is also possible that post-transcriptional changes led to this discrepancy. Thus, these differences in transcription may be cell-line specific. [4].

The data presented here indicate that there is not a synergistic effect of the TGF-β and Wnt signaling pathways in regulating Gli2 and PTHrP transcription. At the promoter level, the Smad binding element (SBE) within the GLI2 promoter is required for full transcriptional activation of GLI2, but the TGF-β inhibitor 2G7 alone did not reduce basal Gli2 mRNA levels in serum-free conditions where autocrine TGF-β signaling levels are low. 2G7 neutralizing activity was confirmed *in vitro* by blocking recombinant TGF-β induction of Gli2 in MDA-MB-231 cells (data not shown), but its activity was not sufficient to inhibit endogenous Gli2. This is in contrast to deletion of the TGF-β type II receptor (TGFBRII), which is sufficient to reduce Gli2 mRNA levels [4]. These data suggest that basal autocrine

TGF-β signaling in these cells is low, but that paracrine TGF-β signaling can activate the TGFBRII and Gli2 transcription. In contrast, the TCF binding element (TCE) was not required for TGF-β stimulation of the GLI2 promoter, but treatment with sclerostin was sufficient to reduce basal Gli2 mRNA levels. These data suggest that the GLI2 promoter may be more sensitive to changes in β-catenin/TCF4 levels downstream of Wnt signaling. We also conclude that TGF-β effects on Gli2 and PTHrP production are likely mediated at least in part through the surrounding stromal cells. Inhibition of TGF-β sor Wnt signaling in either stromal cells or tumor cells effectively abolishes HS5 CM-induced increases in Gli2 and PTHrP. Both Wnt and TGF-β signaling may be involved in stromal cell activation of Gli2 and PTHrP in breast cancer cells, and we show here that Wnt3a secreted by stromal cells drives the stromal-cell induced increase in Gli2 and PTHrP mRNA levels. Importantly, we also demonstrate that β-catenin in tumor cells and Wnt3a secreted by stromal cells are required for stromal cells to enhance osteolytic bone destruction. These data suggest that inhibition of Wnt signaling within the bone microenvironment may block these tumor-enhancing effects by acting on both tumor and stromal cells.

MDA-MB-231 breast cancer cells express low levels of β-catenin in culture [26], but also express very high levels of Dkk1, which is a downstream target of Wnt signaling and an indicator of activated Wnt signaling [31]. Tissue culture plastic, which has rigidity comparable to that of trabecular bone, activated the Wnt reporter TOPflash and elevated mRNA levels of Wnt molecules in breast cancer cells. This suggests that breast cancer cells grown on tissue culture plastic may already be in a Wnt “active” state, which is consistent with their high basal expression of Dkk1 [31] and may in fact provide a mechanism for this elevated expression. Since hyper-activation of downstream Wnt signaling by either forced expression of β-catenin or LiCl treatment enhanced Gli2 and PTHrP transcription in both RWGT2 and MDA-MB-231 cells, the level of Wnt activity in these cells may still be influenced by micro-environmental cues and have not reached a maximal threshold of Wnt activation. The reduction in nuclear β-catenin when mechano-responsive MDA-MB-231 cells were seeded onto compliant substrates suggests that despite exhibiting high baseline Wnt activity these cells still actively respond to integrin-dependent mechanotransduction [10] and may respond to paracrine signals from the reactive stroma in the bone microenvironment.

It is well established that the reactive stroma and cancer-associated fibroblasts (CAFs) promote breast and prostate tumor growth via paracrine signaling at the primary tumor site [32–37], and that these cells serve as a source of Wnt and TGF-β ligands to preserve cancer stem cells [38], promote cancer progression in the primary site [39, 40], and preserve metastatic colonization [14]. CAFs have also been identified as a source of Wnt ligands adjacent to human prostate tumors that drive prostate tumor growth in a TGFβ-Wnt signaling loop [15]. However, these previous studies have assessed Wnt ligands at the mRNA level only. The data presented here indicate for the first time that fibroblastic cells *secrete* detectable levels of Wnt protein, and that Wnt3a promotes breast cancer-induced bone destruction. There is an extensive body of data showing that fibroblasts are also capable of responding to matrix rigidity [41–43], and our preliminary findings suggest that BMSCs seeded onto rigid matrices have a greater capacity to increase Gli2 and PTHrP

mRNA levels in tumor cells than BMSCs seeded onto compliant matrices (data not shown), suggesting the rigid bone microenvironment may promote osteolysis at multiple levels. The data presented here indicate that BMSCs, including fibroblasts, fuel osteolytic bone destruction *in vivo*, potentially by enhancing the production of factors that drive bone destruction such as PTHrP in tumor cells. Our *in vivo* data suggests that targeting Wnt signaling in stromal cells in combination with conventional therapies may prevent tumor-induced bone destruction.

While there are challenges to targeting Wnt therapeutically, understanding its role in promoting tumor growth in bone in conjunction with signaling pathways like Hedgehog and TGF-β is critical, since inhibitors to these co-regulatory pathways are being developed for clinical use [44–47]. The data presented here suggest that inhibition of Wnt signaling in the tumor-bone microenvironment would be highly efficient if it blocked both autocrine and paracrine signaling, but this would likely have serious side effects on bone formation, since Wnt signaling in chondrocytes [48] and osteoblast precursors is required for normal bone formation [49]. The levels of Wnt ligands secreted by stromal cells within the bone marrow, while sufficient to promote tumor-induced bone destruction, did not result in any marked effect on osteoblast numbers within the bone (data not shown), indicating that any potential pro-osteoblast differentiation effects these stromal-secreted Wnts may have within the bone are negligible to the tumor-induced bone destruction. There was also no change in osteoclast numbers when stromal cells were co-inoculated with tumor cells (data not shown), but there is frequently little bone present within the primary spongiosa in these tumor models at endpoint and therefore changes in osteoclast number can be difficult to detect following intratibial inoculation. Surprisingly β-catenin is not required for normal lymphopoiesis and hematopoiesis [50], which suggests that if the therapeutic challenges to disrupting bone formation could be bypassed there may be minimal off target effects in the bone marrow niche; however, the data presented here showing that Smads were able to stimulate Gli2 transcription in the absence of a functional TCF binding site suggest that both Wnt and TGF-β signaling pathways must be blocked to abrogate Gli2 transcription under the control of autocrine mechanisms. In contrast, Wnt blockade using sclerostin completely blocked BMSC-induced Gli2 transcription, suggesting TGF-β signaling is not required for paracrine induction of Gli2 and PTHrP. It is unclear whether both TGF-β and Wnt inhibition may therefore be required to completely eliminate downstream induction of Gli2 and resulting bone destruction *in vivo*, but previous work indicates that TGF-β inhibition *in vivo* partially blocks tumor-induced bone destruction [51], which may be in part due to inhibition of Wnt effects on Gli2 transcription.

In conclusion, the data presented here show that the rigidity of the bone matrix encountered by tumor cells and the surrounding reactive BMSCs promote the induction of PTHrP and its upstream regulator Gli2 and increase tumor-induced osteolysis, and that these processes are in part driven by the Wnt signaling pathway. As the Wnt and TGF-β signaling pathways continue to be developed for clinical use in a variety of cancers, the involvement of these two pathways in the initiation and propagation of bone destruction merits additional monitoring for bone metastases in patients receiving these therapeutic interventions.

Acknowledgements

We wish to thank Dr. T. John Martin for his scientific critiques and guidance, and Dr. Sabrina Danilin for technical support. We would also like to thank Dr. Sylviane Dennler for the generous contribution of the Gli2 WT, mS, and mT promoter constructs. Additionally, we wish to thank MinSung Kim, Shanik Fernando, Barbara Rowland, Denise Buenrostro, and Anne Talley for assistance with the animal experiments.

Funding sources: VA Career Development Award (JAS), VA Merit 1I01BX001957 (JAS), NIH R01CA163499 (SAG/JAS) NIH CA40035-19 (JAS/SAG), CA126505-02 (JAS), AR051639 (JAS), TMEN U54 CA126505 (JAS/SAG/ RWJ), 5T32CA009592-23 (RWJ), VICTR CTSA funding UL1 RR024975-01 (JAS)

References

1. Mundy GR. Mechanisms of bone metastasis. Cancer. 1997; 80 Suppl(8):1546–1556. [PubMed: 9362421]
2. Sterling JA, et al. Advances in the biology of bone metastasis: how the skeleton affects tumor behavior. Bone. 2011; 48(1):6–15. [PubMed: 20643235]
3. Yin JJ, et al. TGF-beta signaling blockade inhibits PTHrP secretion by breast cancer cells and bone metastases development. The Journal of clinical investigation. 1999; 103(2):197–206. [PubMed: 9916131]
4. Johnson RW, et al. TGF-beta promotion of Gli2-induced expression of parathyroid hormone-related protein, an important osteolytic factor in bone metastasis, is independent of canonical Hedgehog signaling. Cancer research. 2011; 71(3):822–831. [PubMed: 21189326]
5. Werkmeister JR, et al. Effect of transforming growth factor-beta1 on parathyroid hormone-related protein secretion and mRNA expression by normal human keratinocytes in vitro. Endocrine. 1998; 8(3):291–299. [PubMed: 9741834]
6. Yu H, Mouw JK, Weaver VM. Forcing form and function: biomechanical regulation of tumor evolution. Trends Cell Biol. 2011; 21(1):47–56. [PubMed: 20870407]
7. Provenzano PP, Keely PJ. Mechanical signaling through the cytoskeleton regulates cell proliferation by coordinated focal adhesion and Rho GTPase signaling. J Cell Sci. 2011; 124(Pt 8):1195–1205. [PubMed: 21444750]
8. Schrader J, et al. Matrix stiffness modulates proliferation, chemotherapeutic response, and dormancy in hepatocellular carcinoma cells. Hepatology. 2011; 53(4):1192–1205. [PubMed: 21442631]
9. Sterling JA, Guelcher SA. Bone structural components regulating sites of tumor metastasis. Curr Osteoporos Rep. 2011; 9(2):89–95. [PubMed: 21424744]
10. Ruppender NS, et al. Matrix rigidity induces osteolytic gene expression of metastatic breast cancer cells. PloS one. 2010; 5(11):e15451. [PubMed: 21085597]
11. Dennler S, et al. Cloning of the human GLI2 Promoter: transcriptional activation by transforming growth factor-beta via SMAD3/beta-catenin cooperation. The Journal of biological chemistry. 2009; 284(46):31523–31531. [PubMed: 19797115]
12. Green JL, et al. Paracrine Wnt signaling both promotes and inhibits human breast tumor growth. Proceedings of the National Academy of Sciences of the United States of America. 2013; 110(17):6991–6996. [PubMed: 23559372]
13. Mukherjee N, et al. Subtype-specific alterations of the Wnt signaling pathway in breast cancer: clinical and prognostic significance. Cancer science. 2012; 103(2):210–220. [PubMed: 22026417]
14. Malanchi I, et al. Interactions between cancer stem cells and their niche govern metastatic colonization. Nature. 2012; 481(7379):85–89. [PubMed: 22158103]
15. Placencio VR, et al. Stromal transforming growth factor-beta signaling mediates prostatic response to androgen ablation by paracrine Wnt activity. Cancer research. 2008; 68(12):4709–4718. [PubMed: 18559517]
16. Luga V, Wrana JL. Tumor-stroma interaction: Revealing fibroblast-secreted exosomes as potent regulators of Wnt-planar cell polarity signaling in cancer metastasis. Cancer research. 2013; 73(23):6843–6847. [PubMed: 24265274]

17. Sterling JA, et al. The hedgehog signaling molecule Gli2 induces parathyroid hormone-related peptide expression and osteolysis in metastatic human breast cancer cells. Cancer research. 2006; 66(15):7548–7553. [PubMed: 16885353]
18. Guise TA, et al. Evidence for a causal role of parathyroid hormone-related protein in the pathogenesis of human breast cancer-mediated osteolysis. The Journal of clinical investigation. 1996; 98(7):1544–1549. [PubMed: 8833902]
19. Guise TA, et al. The combined effect of tumor-produced parathyroid hormone-related protein and transforming growth factor-alpha enhance hypercalcemia in vivo and bone resorption in vitro. The Journal of clinical endocrinology and metabolism. 1993; 77(1):40–45. [PubMed: 8325957]
20. Gallwitz WE, Guise TA, Mundy GR. Guanosine nucleotides inhibit different syndromes of PTHrP excess caused by human cancers in vivo. The Journal of clinical investigation. 2002; 110(10): 1559–1572. [PubMed: 12438453]
21. Jamieson C, Sharma M, Henderson BR. Regulation of beta-Catenin Nuclear Dynamics by GSK-3beta Involves a LEF-1 Positive Feedback Loop. Traffic. 2011
22. Stambolic V, Ruel L, Woodgett JR. Lithium inhibits glycogen synthase kinase-3 activity and mimics wingless signalling in intact cells. Curr Biol. 1996; 6(12):1664–1668. [PubMed: 8994831]
23. Johnson RW, et al. The Primary Function of gp130 Signaling in Osteoblasts is to Maintain bone Formation and Strength, Rather than Promote Osteoclast Formation. Journal of bone and mineral research : the official journal of the American Society for Bone and Mineral Research. 2013
24. Johnson LC, et al. Longitudinal live animal micro-CT allows for quantitative analysis of tumor-induced bone destruction. Bone. 2011; 48(1):141–151. [PubMed: 20685406]
25. Danilin S, et al. Myeloid-derived suppressor cells expand during breast cancer progression and promote tumor-induced bone destruction. Oncoimmunology. 2012; 1(9):1484–1494. [PubMed: 23264895]
26. Klemm F, et al. beta-catenin-independent WNT signaling in basal-like breast cancer and brain metastasis. Carcinogenesis. 2011; 32(3):434–442. [PubMed: 21173432]
27. Letamendia A, Labbe E, Attisano L. Transcriptional regulation by Smads: crosstalk between the TGF-beta and Wnt pathways. J Bone Joint Surg Am. 2001; 83-A Suppl 1(Pt 1):S31–S39. [PubMed: 11263663]
28. Fuxe J, Vincent T, Garcia de Herreros A. Transcriptional crosstalk between TGFbeta and stem cell pathways in tumor cell invasion: Role of EMT promoting Smad complexes. Cell Cycle. 2010; 9(12):2363–2374. [PubMed: 20519943]
29. Lim SK, et al. Tyrosine phosphorylation of transcriptional coactivator WW-domain binding protein 2 regulates estrogen receptor {alpha} function in breast cancer via the Wnt pathway. FASEB J. 2011
30. Previdi S, et al. Interaction between human-breast cancer metastasis and bone microenvironment through activated hepatocyte growth factor/Met and beta-catenin/Wnt pathways. Eur J Cancer. 2010; 46(9):1679–1691. [PubMed: 20350802]
31. Xu WH, et al. Expression of dickkopf-1 and beta-catenin related to the prognosis of breast cancer patients with triple negative phenotype. PloS one. 2012; 7(5):e37624. [PubMed: 22649545]
32. Olumi AF, et al. Carcinoma-associated fibroblasts direct tumor progression of initiated human prostatic epithelium. Cancer research. 1999; 59(19):5002–5011. [PubMed: 10519415]
33. Cheng N, et al. Loss of TGF-beta type II receptor in fibroblasts promotes mammary carcinoma growth and invasion through upregulation of TGF-alpha-, MSP- and HGF-mediated signaling networks. Oncogene. 2005; 24(32):5053–5068. [PubMed: 15856015]
34. Cunha GR, Hayward SW, Wang YZ. Role of stroma in carcinogenesis of the prostate. Differentiation; research in biological diversity. 2002; 9(10):473–485.
35. Hayward SW, et al. Malignant transformation in a nontumorigenic human prostatic epithelial cell line. Cancer research. 2001; 61(22):8135–8142. [PubMed: 11719442]
36. Owens P, et al. Bone Morphogenetic Proteins stimulate mammary fibroblasts to promote mammary carcinoma cell invasion. PloS one. 2013; 8(6):e67533. [PubMed: 23840733]
37. McCart Reed AE, et al. Thrombospondin-4 expression is activated during the stromal response to invasive breast cancer. Virchows Archiv : an international journal of pathology. 2013; 463(4):535–545. [PubMed: 23942617]

38. Nishimura K, et al. Mesenchymal stem cells provide an advantageous tumor microenvironment for the restoration of cancer stem cells. Pathobiology : journal of immunopathology, molecular and cellular biology. 2012; 79(6):290–306.
39. Bacac M, et al. A gene expression signature that distinguishes desmoid tumours from nodular fasciitis. The Journal of pathology. 2006; 208(4):543–553. [PubMed: 16440290]
40. Labbe E, et al. Transcriptional cooperation between the transforming growth factor-beta and Wnt pathways in mammary and intestinal tumorigenesis. Cancer research. 2007; 67(1):75–84. [PubMed: 17210685]
41. Atance J, Yost MJ, Carver W. Influence of the extracellular matrix on the regulation of cardiac fibroblast behavior by mechanical stretch. Journal of cellular physiology. 2004; 200(3):377–386. [PubMed: 15254965]
42. John J, et al. Boundary stiffness regulates fibroblast behavior in collagen gels. Annals of biomedical engineering. 2010; 38(3):658–673. [PubMed: 20012205]
43. Klemm AH, et al. Comparing the mechanical influence of vinculin, focal adhesion kinase and p53 in mouse embryonic fibroblasts. Biochemical and biophysical research communications. 2009; 379(3):799–801. [PubMed: 19126403]
44. Bogdahn U, et al. Targeted therapy for high-grade glioma with the TGF-beta2 inhibitor trabedersen: results of a randomized and controlled phase IIb study. Neuro-oncology. 2011; 13(1): 132–142. [PubMed: 20980335]
45. Chang AL, et al. Expanded access study of patients with advanced basal cell carcinoma treated with the Hedgehog pathway inhibitor, vismodegib. Journal of the American Academy of Dermatology. 2014; 70(1):60–69. [PubMed: 24189279]
46. Hau P, et al. Inhibition of TGF-beta2 with AP 12009 in recurrent malignant gliomas: from preclinical to phase I/II studies. Oligonucleotides. 2007; 17(2):201–212. [PubMed: 17638524]
47. Jimeno A, et al. Phase I study of the Hedgehog pathway inhibitor IPI-926 in adult patients with solid tumors. Clinical cancer research : an official journal of the American Association for Cancer Research. 2013; 19(10):2766–2774. [PubMed: 23575478]
48. Golovchenko S, et al. Deletion of beta catenin in hypertrophic growth plate chondrocytes impairs trabecular bone formation. Bone. 2013; 55(1):102–112. [PubMed: 23567158]
49. Glass DA 2nd, et al. Canonical Wnt signaling in differentiated osteoblasts controls osteoclast differentiation. Developmental cell. 2005; 8(5):751–764. [PubMed: 15866165]
50. Cobas M, et al. Beta-catenin is dispensable for hematopoiesis and lymphopoiesis. The Journal of experimental medicine. 2004; 199(2):221–229. [PubMed: 14718516]
51. Biswas S, et al. Anti-transforming growth factor ss antibody treatment rescues bone loss and prevents breast cancer metastasis to bone. PloS one. 2011; 6(11):e27090. [PubMed: 22096521]

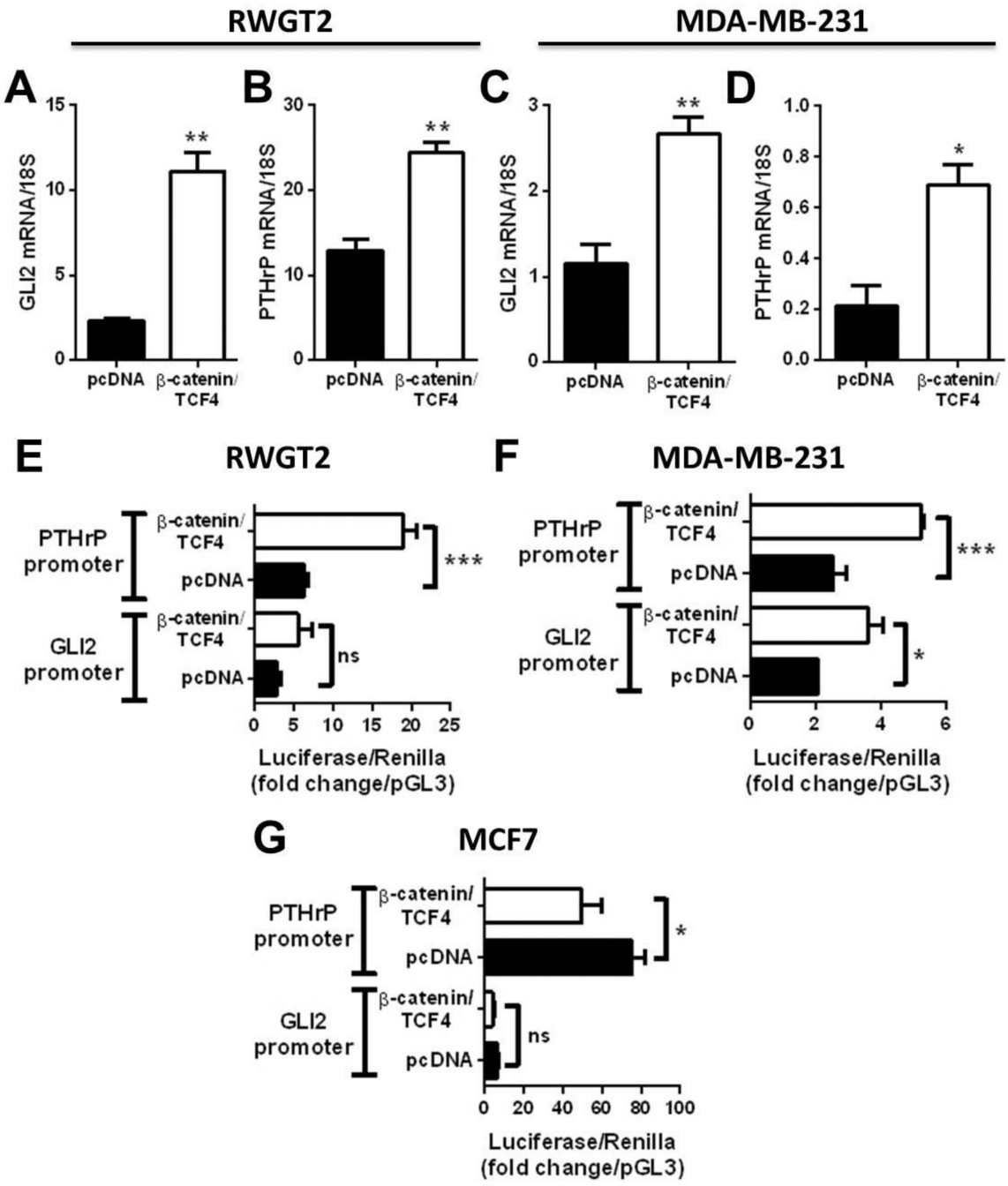

Figure 1. Constitutive β-catenin expression induces Gli2 and PTHrP transcription

(A) Gli2 and (B) PTHrP mRNA levels (expression normalized to 18S eukaryotic rRNA) in RWGT2 osteolytic lung cancer cells and (C,D) MDA-MB-231 cells co-transfected with constitutively expressed β-catenin/TCF4. Gli2 and PTHrP promoter-driven luciferase assay (normalized to Renilla and pGL3 luciferase values) in (E) RWGT2, (F) MDA-MB-231 cells, and (G) MCF7 cells co-transfected with β-catenin/TCF4 constructs. n=3 biological replicates. Graphs represent mean + standard error of the mean, and p-values determined by

unpaired Student's t-test (A–D) and 1-way ANOVA with Tukey Kramer analysis of means (E–G), where *p< 0.05, **p< 0.01, and ***p<0.001.

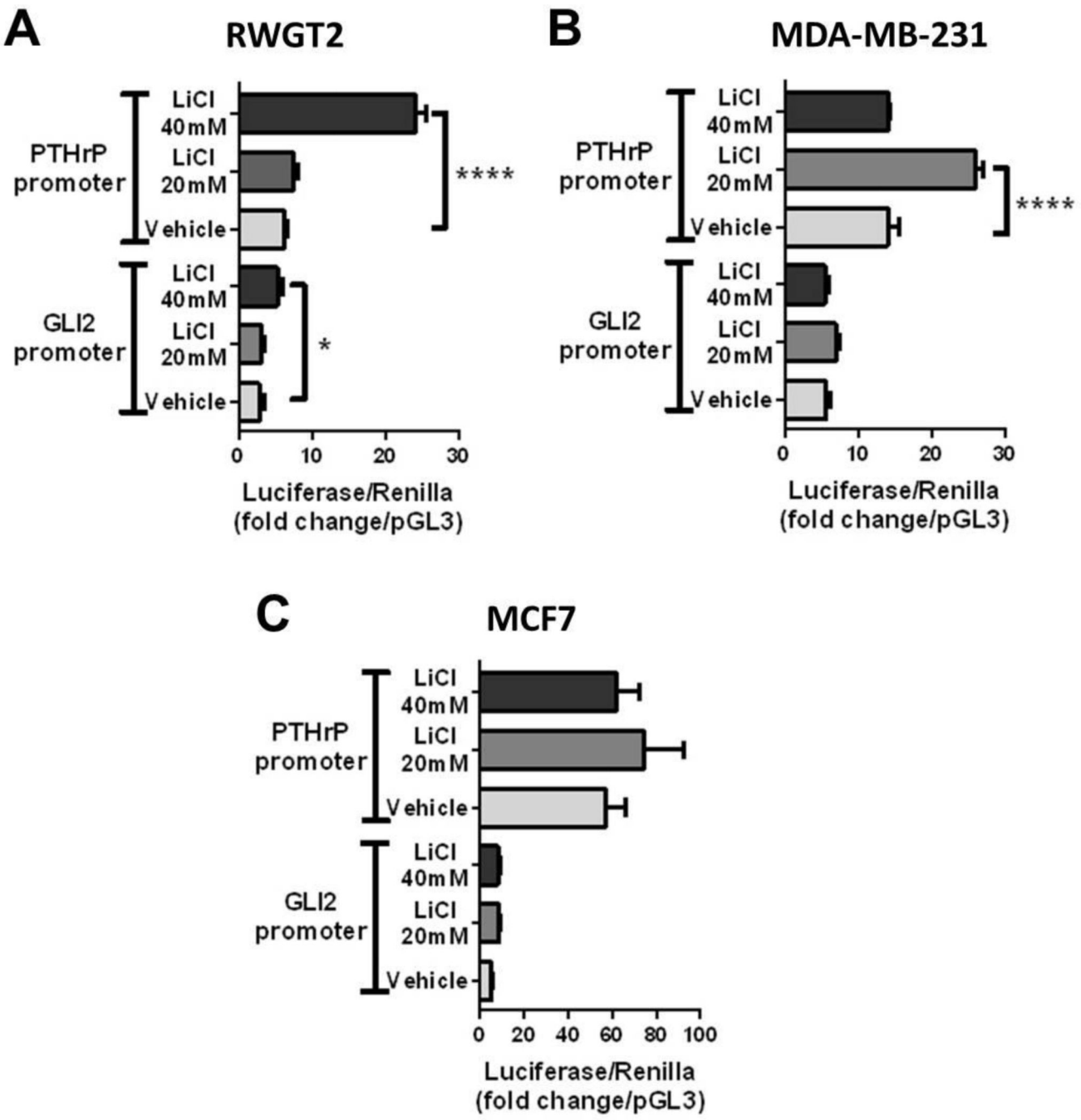

Figure 2. LiCl treatment stimulates Gli2 and PTHrP promoter activation

24 hour treatment with vehicle (water), 20mM, or 40mM LiCl solution in (A) RWGT2, (B) MDA-MB-231, and (C) MCF7 cells transfected with a Gli2 or PTHrP promoter luciferase-reporter construct (normalized to Renilla and pGL3 luciferase values). n=3 biological replicates. Graphs represent mean + standard error of the mean, and p-values determined by 1-way ANOVA with Tukey Kramer analysis of means, where *$p<0.05$ and ****$p<0.0001$.

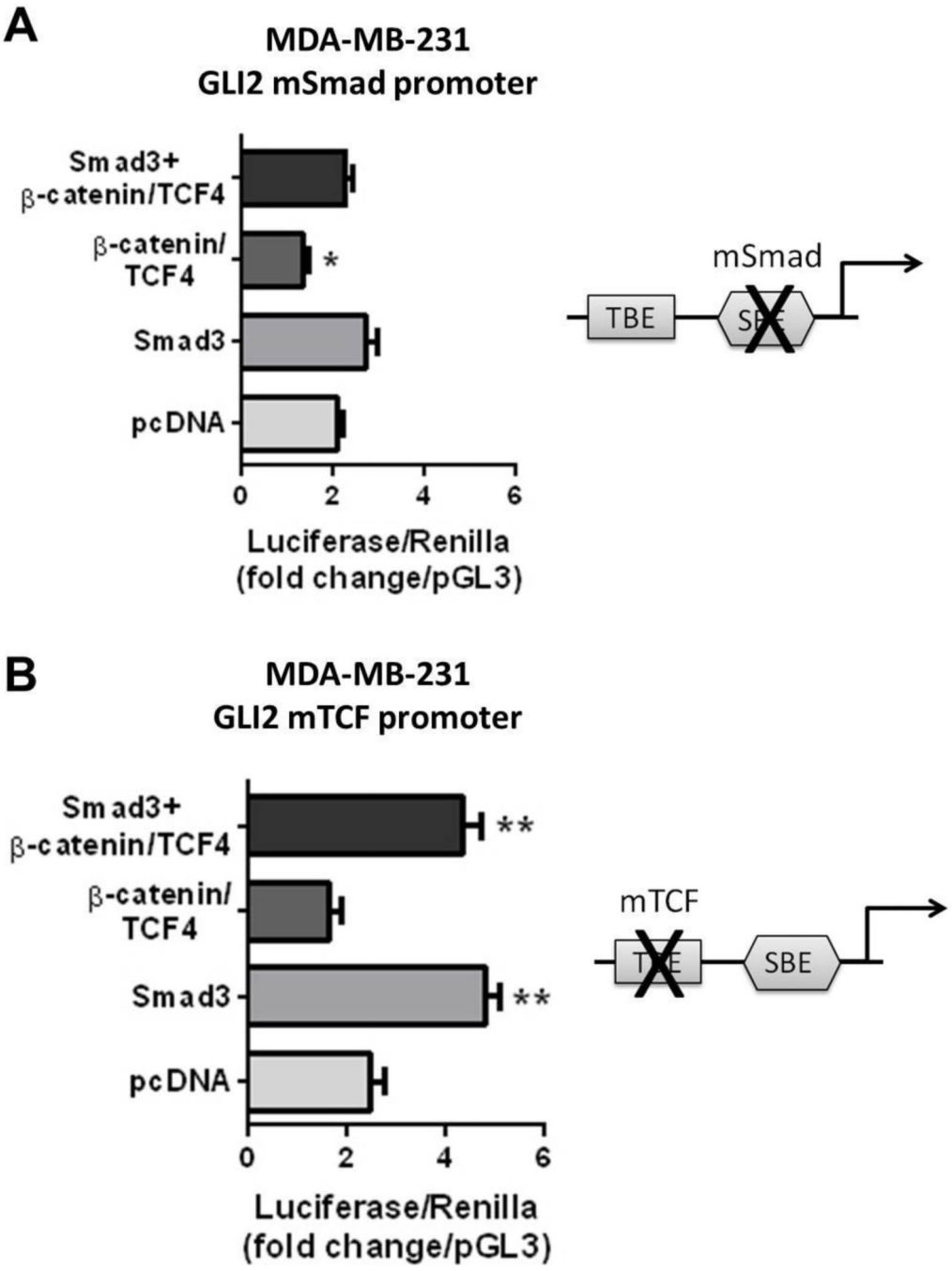

Figure 3. Mutation of transcription factor binding sites in the Gli2 promoter blocks Wnt signaling- mediated Gli2 transcription

MDA-MB-231 cells co-transfected with β-catenin/TCF4/Smad3, β-catenin/TCF4, Smad3, or pcDNA control with (A) mutant Smad (mSmad) or (B) mutant TCF (mTCF) Gli2 promoter luciferase-reporter construct (normalized to Renilla and pGL3 luciferase values). n=3 biological replicates. Graphs represent mean + standard error of the mean, and p-values determined by 1-way ANOVA with Tukey Kramer analysis of means, where *$p<0.05$ and **$p<0.01$ *versus* pcDNA control.

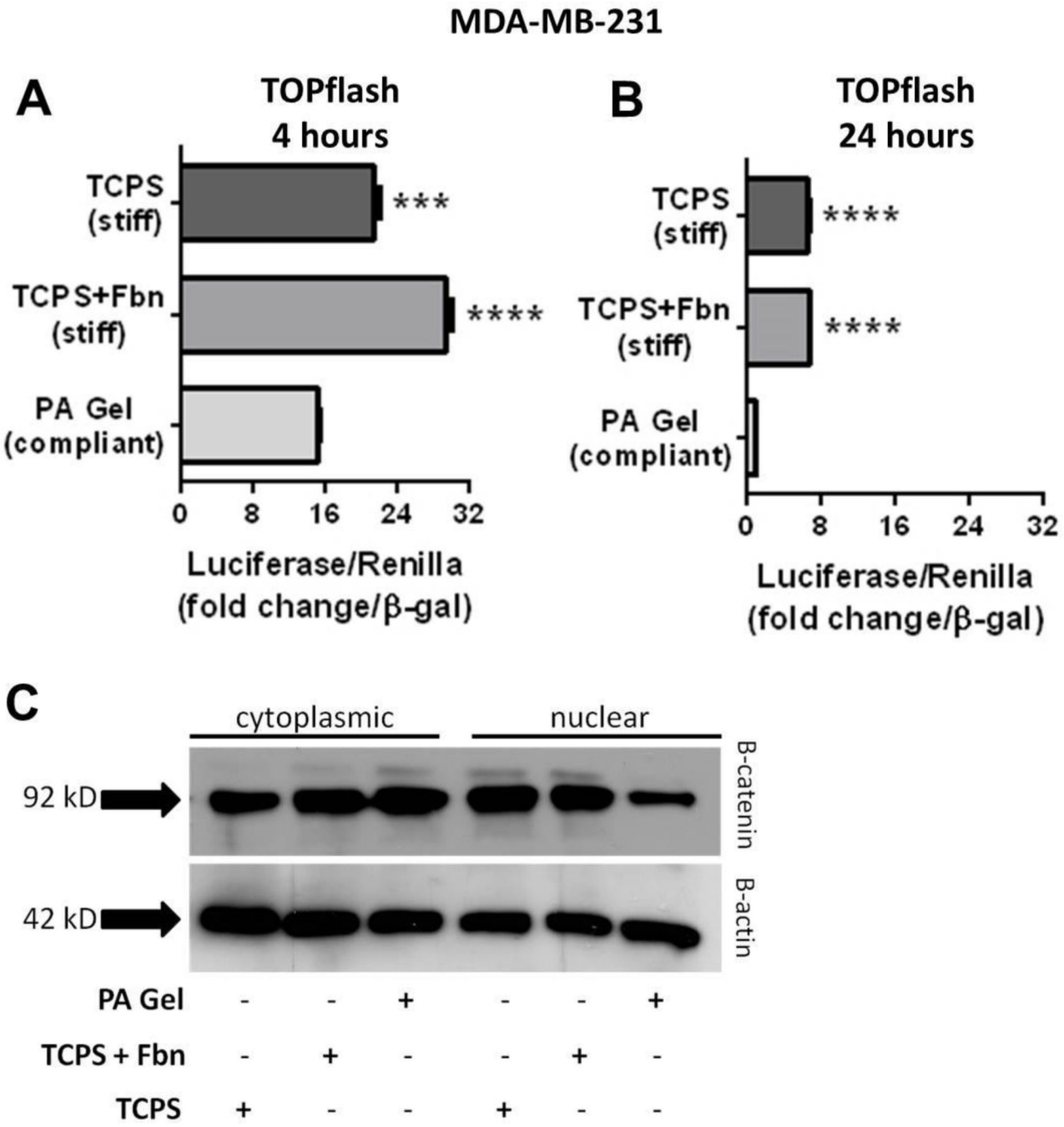

Figure 4. Rigidity activates Wnt signaling in breast cancer cells and induces nuclear β-catenin accumulation

MDA-MB-231 cells transfected with TOPFlash luciferase-reporter construct and seeded onto tissue culture polysterene (TCPS) without fibronectin (Fbn), TCPS+Fbn, or polyacrylamide (PA) gel substrates for (A) 4 hours and (B) 24 hours. (C) Western blot for β-catenin accumulation in cytoplasmic and nuclear fractions of MDA-MB-231 cells seeded onto TCPS, TCPS+Fbn, or PA gel for 24 hours. n=3 biological replicates and Western blot representative of 3 biological replicates. Graphs represent mean + standard error of the

mean, and p-values determined by 1-way ANOVA with Tukey Kramer analysis of means, where ***p<0.001 and ****p<0.0001.

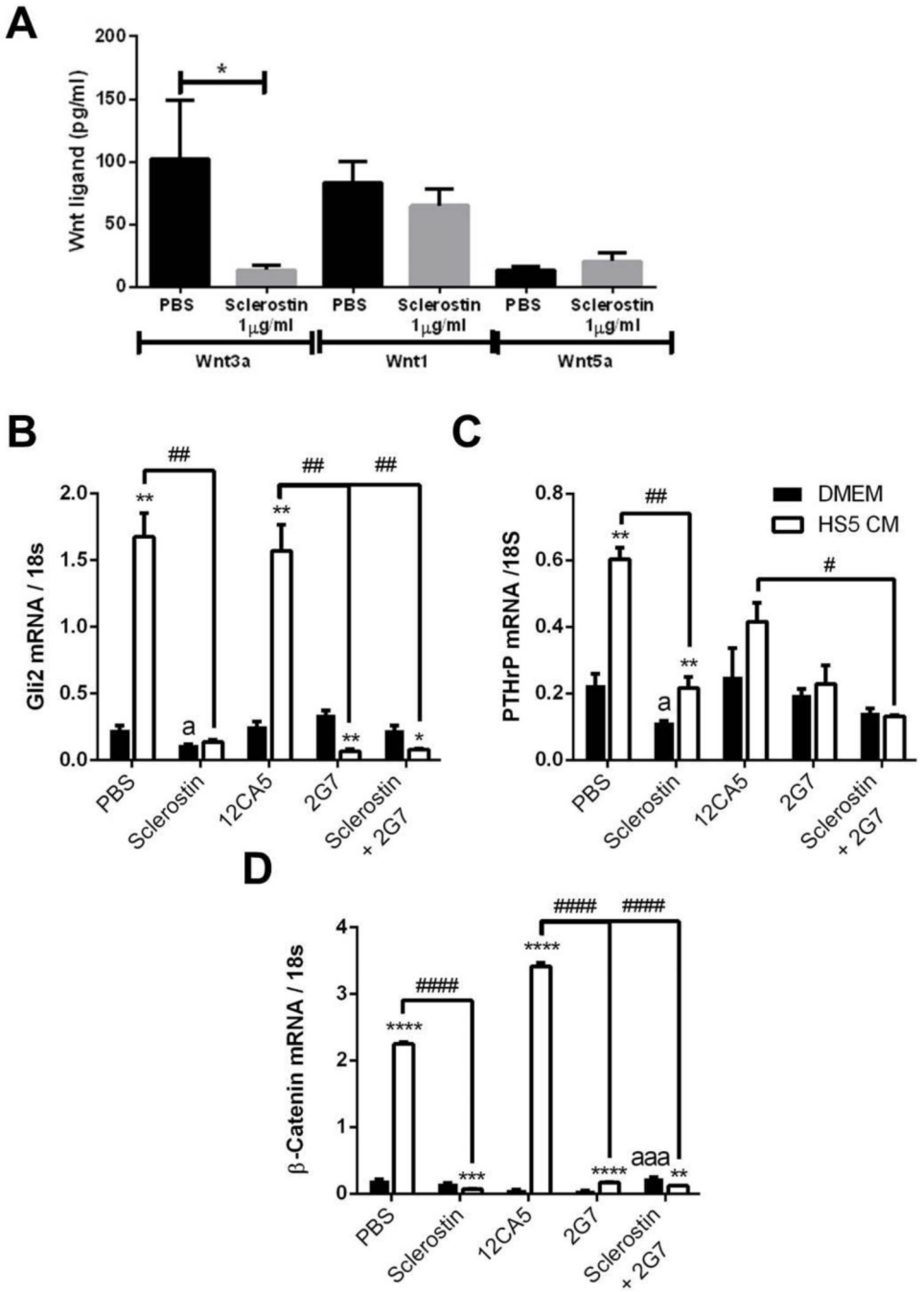

Figure 5. Stromal-secreted Wnt and TGF-β signaling factors enhance Gli2 and PTHrP mRNA levels

(A) ELISA for secreted levels of canonical (Wnt3a, Wnt1) and non-canonical (Wnt5a) Wnt proteins in the conditioned media from HS5 human bone marrow stromal cells following 24 hour treatment with vehicle (PBS) or sclerostin (1.5μg/ml). (B–D) MDA-MB-231 cells cultured for 24 hours in DMEM + vehicle, sclerostin (1.5μg/ml), 12CA5 control IgG (10μg/ml) or 2G7 (TGF-β neutralizing antibody, 10μg/ml) for 24 hours or in HS5-conditioned media (CM) with vehicle, sclerostin (1.5μg/ml), 12CA5 control IgG (10μg/ml) or 2G7 (TGF-β neutralizing antibody, 10μg/ml) treatment added to the HS5 cells in culture

for 24 hours prior to CM collection. (B) Gli2 (C) PTHrP, and (D) β-catenin mRNA levels normalized to 18S eukaryotic rRNA. n=3 biological replicates, and graphs represent mean + standard error of the mean, and p-values determined by 1-way ANOVA with Tukey Kramer analysis of means. *p<0.05, **p<0.01, ***p<0.001, and ****p<0.0001 *versus* PBS (for A) and *versus* DMEM (for B–D). ^{a}p<0.05, ^{aaa}p<0.001 *versus* PBS or antibody-treated control in DMEM (for B–D). #p<0.05, ##p<0.01, and ####p<0.0001 *versus* PBS or antibody-treated control in HS5 CM (for B–D).

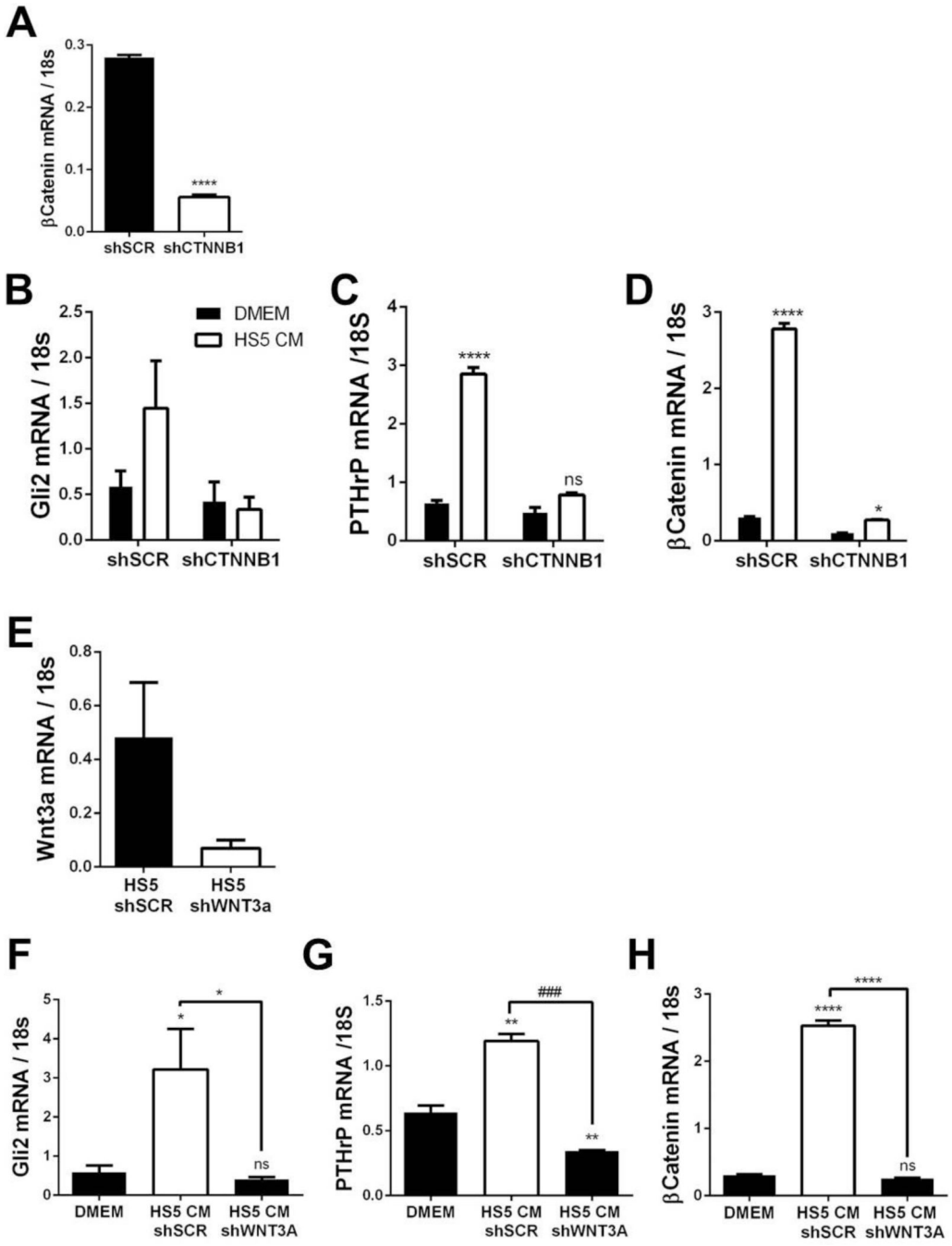

Figure 6. Inhibition of Wnt signaling in tumor or stromal cells blocks stromal cell-mediated increases in Gli2 and PTHrP mRNA levels

(A) β-catenin (CTNNB1) mRNA levels in MDA-MB-231 cells following shRNA-mediated knockdown. (B) Gli2, (C) PTHrP, and (D) β-catenin mRNA levels in MDA-MB-231 scrambled control cells (shSCR) or MDA-MB-231 cells with β-catenin knockdown (shCTNNB1) cultured in DMEM or HS5 conditioned media (CM). (E) Wnt3a mRNA levels in HS5 cells following shRNA-mediated knockdown. (F) Gli2, (G) PTHrP, and (H) β-catenin mRNA levels in MDA-MB-231 cells cultured in CM from HS5 scrambled control cells (HS5 shSCR) or HS5 cells with WNT3a knockdown (shWNT3a). n=3 biological

replicates. Graphs represent mean + standard error of the mean, and p-values determined by unpaired Student's t-test (A & E) or 1-way ANOVA with Tukey Kramer analysis of means (B–D & F–H), where *p<0.05, **p<0.01, and ****p<0.0001 *versus* DMEM. ###p<0.001 *versus* HS5 shSCR.

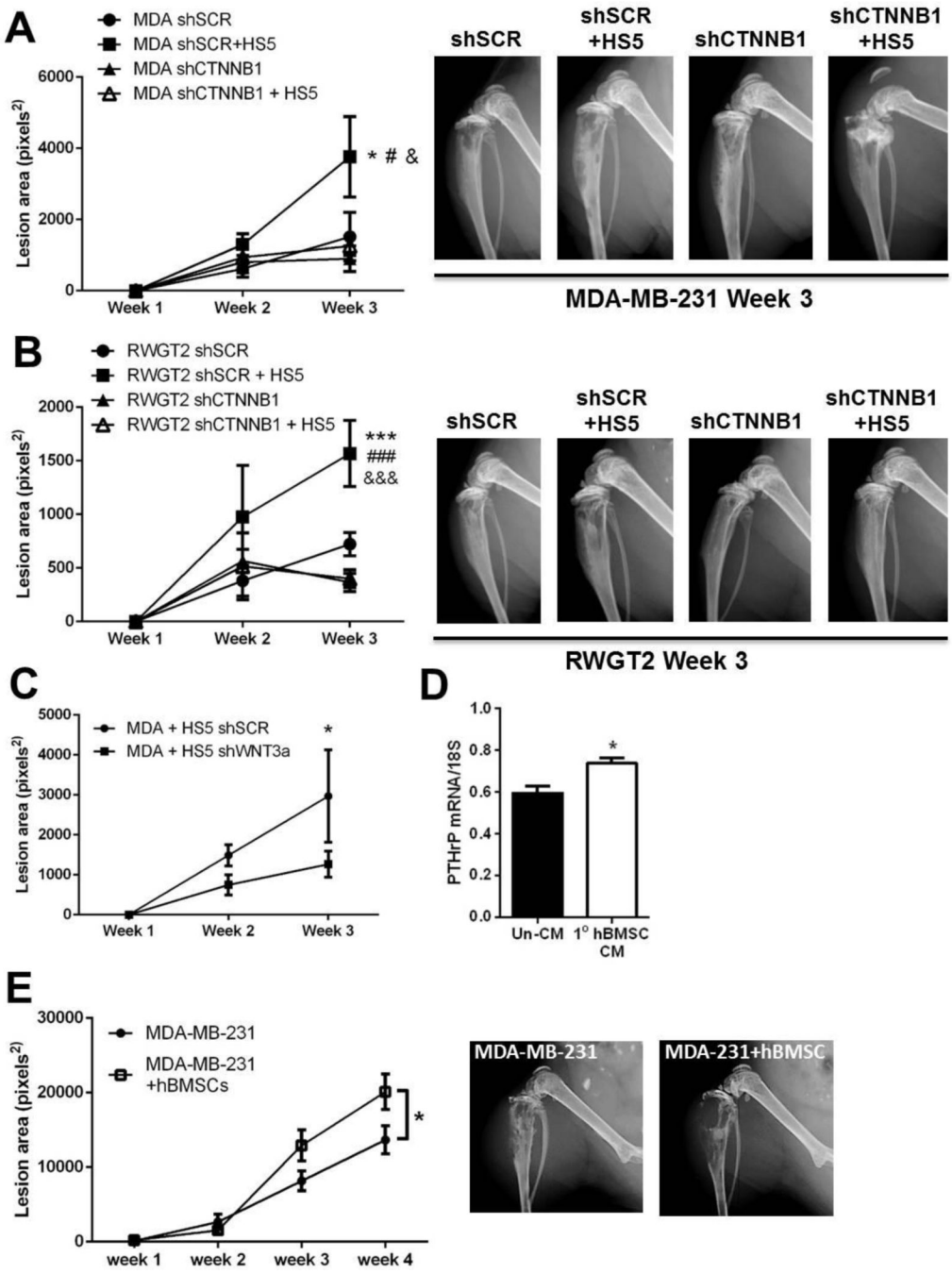

Figure 7. Stromal cell promotion of tumor-induced osteolysis is dependent on Wnt signaling

(A) Osteolytic lesion area (average/group) at weeks 1–3 as determined by ROI analysis following intratibial inoculation of MDA-MB-231 scrambled control cells (shSCR) or MDA-MB-231 cells with β-catenin knockdown (shCTNNB1) alone or in combination with HS5 stromal cells. n=8/group. *p<0.05 *vs* MDA shSCR, #p<0.05 *vs* MDA shCTNNB1, &p<0.05 *vs* MDA shCTNNB1 + HS5 by 1-way ANOVA with Tukey Kramer analysis of means. (B) Osteolytic lesion area (average/group) at weeks 1–3 as determined by ROI analysis following intratibial inoculation of RWGT2 scrambled control cells (shSCR) or

RWGT2 cells with β-catenin knockdown (shCTNNB1) alone or in combination with HS5 stromal cells. n=8/group. ***p<0.05 *vs* RWGT2 shSCR, ###p<0.05 *vs* RWGT2 shCTNNB1, &&&p<0.05 *vs* RWGT2 shCTNNB1 + HS5 by 1-way ANOVA with Tukey Kramer analysis of means. (C) Osteolytic lesion area (average/group) at weeks 1–3 as determined by ROI analysis following intratibial inoculation of MDA-MB-231 cells in combination with HS5 scrambled control (shSCR) stromal cells or HS5 cells with WNT3a knockdown (shWNT3a). n=8/group. *p<0.05 *vs* MDA + HS5 shWNT3a at week 3 by 1-way ANOVA with Sidak analysis of means. (D) PTHrP mRNA levels in MDA-MB-231 cells cultured in DMEM or conditioned media (CM) from primary human bone marrow stromal cells for 24 hours. n=3 replicates, and *p<0.05 by unpaired Student's t-test. (E) Osteolytic lesion area (average/group) at weeks 1–4 as determined by ROI analysis following intratibial inoculation of MDA-MB-231 cells alone or in combination with primary human bone marrow stromal cells (hBMSCs). n=7–9 mice/group. *p<0.05 by 1-way ANOVA with Tukey Kramer analysis of means. For all graphs, data represent average/group + standard error of the mean.

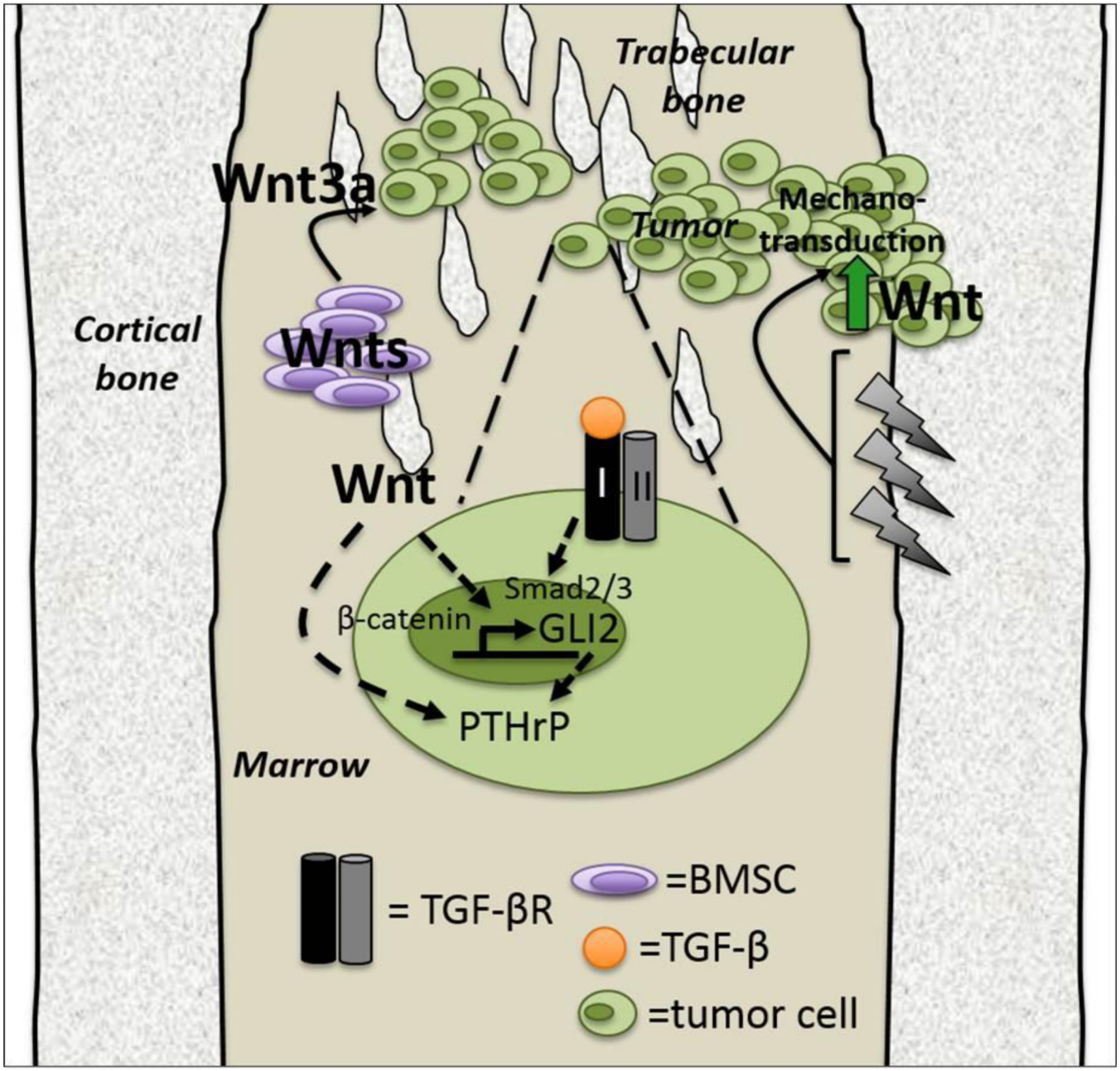

Figure 8. Wnt induces Gli2 and PTHrP in osteolytic tumor cells

Tumor cells (green) in the bone microenvironment sense the rigidity of the bone (gray) via mechanotransduction (lightning bolts), which induces Wnt signaling and an accumulation of nuclear B-catenin in tumor cells. This drives the transcription of Gli2 and PTHrP and facilitates tumor cell growth in the bone. Additionally, bone marrow stromal cells (BMSCs, purple) secrete Wnt ligands (including Wnt3a) that drive Gli2 and PTHrP transcription in disseminated tumor cells. Wnt signaling induction of Gli2 transcription is dependent upon downstream TGF-β signaling molecules Smads 2 and 3. TGF-β = transforming growth factor-beta, BMSC = bone marrow stromal cells.

Table 1

Wnt signaling PCR-based microarray.

Gene family	Gene name	PCR micro-array	SYBR green PCR validation	SYBR Catolog #
Canonical Wnt signaling	DIXDC1	**+5.3**	**+3.1**	QT00019481
	FZD8	**+4.3**	**+4.3**	QT00212128
	DVL1	**+3**	**+1.7**	QT00012663
	FZD3	**+2.8**	**+2**	QT00009114
	FZD4	**+2.7**	**+1.9**	QT00200984
	FZD6	**+1.9**	**+1.1**	QT00047670
	FZD7	−2.3	−1.3	QT00213850
	AXIN1	−1.2	−1.8	QT00076202
	DVL2	−1.2	−2.9	QT00019810
Protein ubiquitination	BTRC (β-TrCP)	**+11.1**	**+2.5**	QT00080787
	FBXW2	**+8.9**	**+2.3**	QT00078225
	FBXW11	**+3.3**	**+2.3**	QT00083251
	FBXW4	**+1.5**	**+2.9**	QT00088123
Non-canonical Wnt signaling	WNT5B	**+8.9**	nd	QT00033558
	WNT5A	**+2.4**	**+4**	QT00025109
	WNT16	**+2.2**	nd	QT00048447
	WNT4	−2.5	nd	QT00041391
	WNT10A	−1.6	**+1.5**	QT00205632
	WNT3	−1.4	−2.9	QT00222698

MDA-MB-231 cells were seeded onto a stiff substrate (TCPS+Fbn) or soft substrate (PA Gel) and harvested for use in a Wnt signaling PCR-based microarray. Genes that were increased (plus sign and bold font) or decreased (minus sign) more than 1.2-fold on TCPS+Fbn *versus* PA Gel are presented above. Data are presented as fold-change differences in mRNA levels. PCR micro-array data are in the left column and PCR validation with SYBR green primers is in the right column. The far right column lists the catalog numbers for the commercial SYBR primers used to validate the PCR micro-array. n=3 biological replicates for micro-array and for SYBR green validation.